Molecular Therapy
Methods & Clinical Development
Original Article

Selective B cell depletion upon intravenous infusion of replication-incompetent anti-CD19 CAR lentivirus

Craig M. Rive,[1] Eric Yung,[1] Lisa Dreolini,[1] Scott D. Brown,[1] Christopher G. May,[1] Daniel J. Woodsworth,[1] and Robert A. Holt[1,2,3]

[1]Canada's Michael Smith Genome Sciences Centre, BC Cancer, Vancouver, BC V5Z 1L3, Canada; [2]Department of Medical Genetics, University of British Columbia, Vancouver, BC V6T 1Z4, Canada; [3]Molecular Biology & Biochemistry, Simon Fraser University, Burnaby, BC V5A 1S6, Canada

Anti-CD19 chimeric antigen receptor (CAR)-T therapy for B cell malignancies has shown clinical success, but a major limitation is the logistical complexity and high cost of manufacturing autologous cell products. If engineered for improved safety, direct infusion of viral gene transfer vectors to initiate *in vivo* CAR-T transduction, expansion, and anti-tumor activity could provide an alternative, universal approach. To explore this approach we administered approximately 20 million replication-incompetent vesicular stomatitis virus G protein (VSV-G) lentiviral particles carrying an anti-CD19CAR-2A-GFP transgene comprising either an FMC63 (human) or 1D3 (murine) anti-CD19 binding domain, or a GFP-only control transgene, to wild-type C57BL/6 mice by tail vein infusion. The dynamics of immune cell subsets isolated from peripheral blood were monitored at weekly intervals. We saw emergence of a persistent CAR-transduced $CD3^+$ T cell population beginning week 3–4 that reaching a maximum of 13.5% ± 0.58% (mean ± SD) and 7.8% ± 0.76% of the peripheral blood $CD3^+$ T cell population in mice infused with ID3-CAR or FMC63-CAR lentivector, respectively, followed by a rapid decline in each case of the B cell content of peripheral blood. Complete B cell aplasia was apparent by week 5 and was sustained until the end of the protocol (week 8). No significant CAR-positive populations were observed within other immune cell subsets or other tissues. These results indicate that direct intravenous infusion of conventional VSV-G-pseudotyped lentiviral particles carrying a CD19 CAR transgene can transduce T cells that then fully ablate endogenous B cells in wild-type mice.

INTRODUCTION

Ordinarily, a cancer patient's immune system can recognize cancer cells as being altered and mount a natural immune response. T cells are known to be the main mediators of the anti-cancer immune response, but sometimes the natural T cell response is ineffective; T cells may fail to recognize tumor cells, fail to activate, or fail to sustain a response long enough to have an impact. It is possible for these limitations to be overcome by genetic engineering strategies that involve isolating a sample of a patient's T lymphocytes, genetically modifying and activating the cells *ex vivo*, and then re-administering them to the same patient. The genetic modification step involves introducing into the T cells an extra gene that carries instructions for a new antigen receptor that may be, for example, a recombinant alpha-beta T cell receptor (αβTCR) or a chimeric antigen receptor (CAR). Much of the growing interest in genetically engineered immune effector cells (IECs) as a new class of therapeutic is driven by the impressive results CAR-T therapies have shown in patients with relapsed/refractory B cell acute lymphoblastic leukemia or non-Hodgkin's lymphoma. These patients, for whom standard therapies have failed, have historically had dismal outcomes with survival measured in weeks or months. Remarkably, CAR-T therapy targeting CD19 has led to meaningful and durable remissions for a large proportion of these patients in many different studies.[1–7]

Currently, most genetically engineered IEC therapies require several steps, including (1) manufacturing plasmid encoding the synthetic transgene and ancillary plasmids, (2) delivery of these plasmids into producer cells to generate virus, (3) collection of patient autologous T cells and integration of the transgene into the genomes of these cells by viral transduction, (4) expansion of the transduced T cells *ex vivo* to produce the therapeutic cells, (5) extensive release testing of the manufactured product, (6) preconditioning lymphodepletion of the patient, (7) infusion of the modified autologous cells, and (8) intensive clinical and immunological monitoring. Thus, there is considerable infrastructure and expertise required to deliver IEC treatments safely and successfully. The complexity of manufacturing IECs is a critical limitation to the cell therapy field, and a major contributor to the high cost of new cell-based interventions coming to market. Hence, there is considerable interest in the potential for a universal alternative to autologous CAR-T products, with some encouraging results seen from gene-edited allo-CAR-Ts pre-clinically[8] and in case studies.[9,10] Likewise, the immortalized IEC cell line natural killer

Received 22 May 2021; accepted 25 May 2022;
https://doi.org/10.1016/j.omtm.2022.05.006.

Correspondence: Robert A. Holt, PhD, Canada's Michael Smith Genome Sciences Centre, BC Cancer, Vancouver, BC V5Z 1L3, Canada.
E-mail: rholt@bcgsc.ca

(NK)-92 has shown encouraging safety and efficacy in a recent phase 1 trial, but the requirement of irradiating the cells pre-infusion to reduce oncogenic risk will likely remain limiting for this approach.[11] The generation of a bank of allogeneic CAR-T cells by *in vitro* differentiation and maturation of hematopoietic stem and progenitor cell precursors is an alternative and highly compelling strategy. Demonstrated in principle, this approach awaits further optimization.[12]

In principle, universal IEC therapy could also be achieved by direct infusion of a gene transfer vector, such that cell manufacturing is sidestepped completely. Different approaches to *in vivo* gene delivery have been explored, preclinically, for CAR-T therapy. Nanoparticles that carry a CAR transposon and that are coated with anti-CD3 targeting antibodies can transduce T cells *in vivo* yielding functional CAR-T cells,[13] as can lipid nanoparticles that carry CAR mRNA and display anti-CD5 targeting antibodies.[14] Similarly, *in vivo* delivery of high doses of 10^{10} to 10^{11} lentiviral particles that bear CAR transgenes, and that have been pseudotyped to target either CD3+, CD8+, or CD4+ T cells, can yield functional CAR-T.[15–17] Here, we show efficient *in vivo* generation of functional CAR-T cells in wild-type mice upon infusion of lower doses (on the order of 10^6 to 10^7 particles) of conventional VSV-G lentivirus bearing transgenes that encode conventional FMC63 or ID3 anti-CD19 binding domains.

RESULTS

During our early pre-clinical development of an anti-CD19 CAR intervention for B cell malignancies, we explored how CAR-T cells behave *in vitro* in the context of antigen-driven expansion. Using a standard second-generation anti-CD19 CAR design[18] (EF1α promoter, FMC63 scFv CD19 binding domain, CD8α hinge and transmembrane domain, 4-1BB co-stimulatory domain, CD3z signaling domain, and 2A-GFP tag), we observed, as have many other investigators, that B cells drive robust expansion of functional CD19 CAR-T cells *in vitro*. This led us to explore *in vivo* transduction and expansion of CAR-T cells *in vivo* using a murine model system. We constructed a CAR where we changed the scFv binding domain from FMC63[19] (a monoclonal antibody raised against human CD19) to 1D3[20] (a monoclonal antibody raised against mouse CD19). To verify activity *in vitro*, 2.5×10^5 splenocytes from wild-type C57BL/6 mice were transduced with lentivirus encoding either the 1D3-CD19CAR-GFP (murine), FMC63-CD19CAR-GFP (human), or GFP-only transgene, then stimulated with a further excess of irradiated autologous murine splenocytes as a source of murine CD19 antigen. We observed that murine T cells modified with either of the CARs expanded rapidly and selectively. Specifically, for murine T cells modified with the human CAR, expansion was 8.8-fold ± 0.03-fold (mean ± standard deviation [SD]) at day 63 relative to GFP-transduced T cells ($p < 0.004$, paired two-tail t test), and for murine T cells modified with the murine CAR, expansion was 12.9-fold ± 0.09-fold at day 63, relative to GFP-transduced T cells ($p < 0.002$, paired two-tail t test). The murine control T cells transduced with GFP-only lentivirus showed very limited yet detectable expansion, possibly driven by the original CD3/CD28 activation prior to transduction (Figures 1A and 1B). All expanded murine CAR-T cells showed robust and selective killing of murine B cells *in vitro*. Target murine B cells co-cultured with either effector 1D3-CD19CAR-GFP or FMC63-CD19CAR-GFP modified murine T cells showed 24.8% ± 1.69% (mean ± SD) and 18.5% ± 1.08% of murine B cells were unviable (FVS780 positive) after the 5-h co-culture, respectively (Figure 1C).

For further validation, we used 1D3 and FMC63 CD19-blocking antibodies to assess murine CAR-T cell specificity for the mouse CD19 antigen expressed by the A20 cell line (Figure 1D). As a baseline, 38.8% ± 0.71% (mean ± SD) of the target A20 cells were unviable after a 4-h co-culture with the effector 1D3-CD19CAR-GFP modified murine T cells with no blocking antibody present. Upon titration of 1D3-blocking antibody, the ability of the 1D3-CD19CAR-GFP modified murine T cells to target the A20 cells produced a decrease in unviable A20 cells to 19.7% ± 0.28% (mean ± SD), which was the level of background killing observed for murine T cells transduced with the GFP-only transgene, likely due to alloreactivity. Likewise, 41.1% ± 0.92% (mean ± SD) of the target A20 cells were unviable after a 4-h co-culture the effector FMC63-CD19CAR-GFP modified murine T cells with no blocking antibody present and 20.8% ± 0.57% of the A20 cells upon titration of FMC63 antibody. Interestingly, these results confirm that the FMC63 scFv is able to bind murine CD19 to the degree necessary for functional CAR-T activation in this experimental system. To our knowledge, this has not previously been reported.

We then administered lentivirus encoding each CAR or GFP-only lentivirus to C57B/6 wild-type mice (age 6–8 weeks) by tail vein infusion, and drew peripheral blood at regular intervals. For the following experiments, the number of mice per treatment group was eight (n = 8). In Figures 2 and 3, error bars represent the SD away from the calculated mean of each treatment group. We observed that GFP-expressing T cells appear in the blood of mice 3 weeks after the initial injection of $3.6–4 \times 10^6$ infectious units (IU) of either the 1D3-or FMC63-CD19CAR-GFP lentivirus, but not after injection of the same dose of GFP-only lentivirus (Figure 2). Specifically, we saw emergence of a persistent 1D3-CD19CAR-GFP-transduced $CD3^+$ T cell population beginning at week 3 that reaching a maximum of 13.5% ± 0.58% (mean ± SD) of the peripheral blood $CD3^+$ T cell population by week 5 (Figures 2A–2C). This coincided with the loss of B cells, seen 5 weeks after the initial injection (Figure 2C). In experiments where we infused murine T cells modified with the FMC63-CD19CAR-GFP construct, we also saw the emergence of a persistent FMC63-CD19CAR-GFP-transduced $CD3^+$ T cell population beginning at week 5 that reached a maximum of 7.8% ± 0.76% of the peripheral blood $CD3^+$ T cell population by week 5 (Figures 2A–2C). Again, this coincided with a loss of B cells, seen 5 weeks after the initial injection. This further confirms functional recognition of murine CD19 by FMC63 (Figure 2C). With either CAR, B cell aplasia was sustained until the end of the protocol (week 8). Mice treated with $3.6–4 \times 10^6$ IU of the GFP control lentivirus had no GFP-expressing T cells and did not show the same B cell loss (Figures 2A–2C). We looked for GFP expression in immune cell subsets other than T cells, including the CD20/CD45R/B220 B cell population,

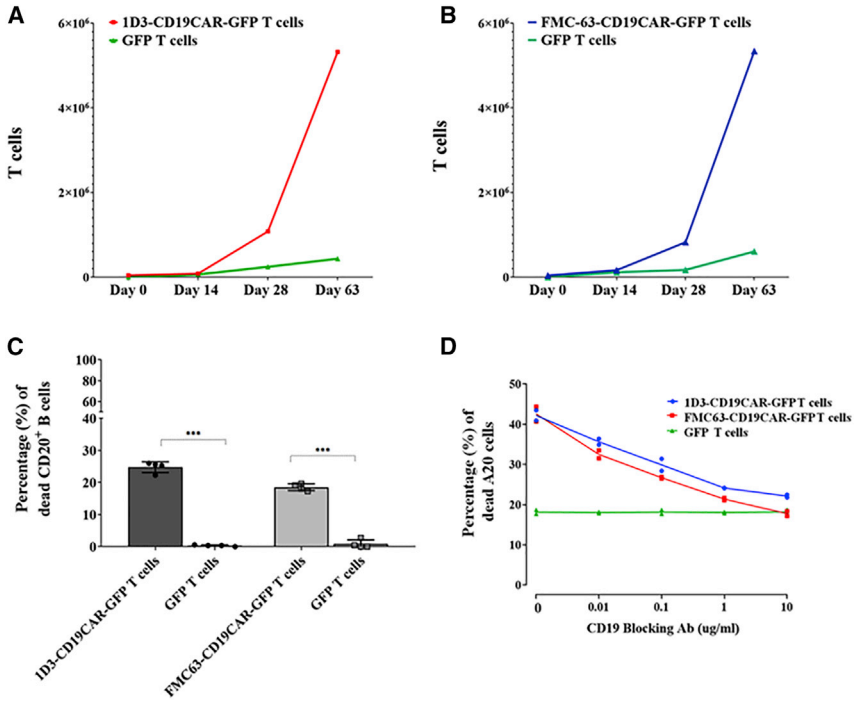

Figure 1. *In vitro* proliferation and cytolytic activity of murine CAR-T cells

(A) 2.5 × 10^5 C57BL/6 splenocytes were transduced with 1D3-CD19CAR-GFP or GFP-only lentivirus at an MOI of 5. The transduced splenocytes were then co-cultured with an excess of irradiated C57BL/6 splenocytes, which provided a source of B cells expressing the CD19 antigen. The 1D3-CD19CAR transduced splenocytes showed a 12.2-fold ± 0.09-fold (mean ± SD) expansion (red, square), compared with GFP transduced (green, triangle) ($p < 0.002$, paired two-tailed t test). (B) 2.5 × 10^5 C57BL/6 splenocytes were transduced with the FMC63-CD19CAR-GFP or GFP-only lentivirus at an MOI of 5. Splenocytes were then co-cultured with irradiated C57BL/6 splenocytes, which provided a source of B cells expressing the CD19 antigen. The FMC63-CD19CAR transduced splenocytes showed an 8.8-fold ± 0.03-fold expansion (orange, square), compared with GFP transduced (cyan, triangle), ($p < 0.004$, paired two-tailed t test). (C) 1 × 10^5 FMC63-CD19CAR-GFP or 1D3-CD19CAR murine T cells from day 63 of the expansion assays were co-cultured for 5 h with target B cells, isolated from C57BL/6 splenocytes, at an E:T ratio of 1:1. Unviable target murine B cells were measured through the shift in the FVS780 signal, measured by flow cytometry (Figure S4). Expanded murine 1D3-CAR-T cells showed robust and selective targeting of murine B cells, with 24.8% ± 1.69% of B cells being unviable after a 5-h co-culture. The FMC63-CD19CAR T cells also showed robust and selective targeting of murine B cells, with 18.5% ± 1.08% of B cells being unviable after a 5-h co-culture. Two-way ANOVA, Sidak's multiple comparison ***$p < 0.002$. (D) 1D3-, FMC63-CD19CAR-, and GFP-transduced and expanded murine T cells were co-cultured with target A20 cells for 4 h. The CD19 antigen on the A20 cells were blocked with either the CD19 1D3 or FMC63-blocking antibody at a starting concentration of 10 μg/mL decreasing 10-fold down to 0 μg/mL, at an E:T ratio of 4:1. Using flow cytometry, target cell death was measured through the shift in the FVS780 signal (Figure S3 and Table S1). The murine CAR-T cells showed robust and selective response when co-cultured with A20 cells. This response decreased with increasing CD19-blocking antibody concentration. 38.8% ± 0.71% of unblocked A20 cells were unviable when co-cultured with the 1D3-CD19CAR T cells, which decreased to 19.7% ± 0.28% of A20 cells blocked with 10 μg/mL of 1D3-CD19-blocking antibody. 41.1% ± 0.92% of unblocked A20 cells were unviable when co-cultured with the FMC63-CD19CAR T cells, which decreased to 20.8% ± 0.57% of A20 cells blocked with 10 μg/mL of FMC63-CD19. Two-way ANOVA $p = 0.04$. Nonlinear regression analysis (sigmoidal) analysis of 1D3-CD19CAR T cells versus A20 CD19-blocking antibody dose response, $R^2 = 0.95$. FMC63-CD19CAR T cells versus A20 CD19-blocking antibody dose response, $R^2 = 0.96$. GFP versus A20 CD19-blocking antibody dose response, $R^2 = 0.01$.

$CD11b^+$ macrophage, and $CD335^+$ NK cells, but found that only T cells expressed the reporter GFP gene, indicative of CAR expression (Figures 2D and 2E). Our interpretation of these results is that interaction between the *in vivo* transduced CAR-T cells and endogenous B cells drives CAR-T cell expansion and CAR-T-mediated B cell depletion, resulting eventually in B cell aplasia. The only overt change to mice treated with either 1D3-or FMC63-CD19CAR lentivirus was a modest decrease in weight of 5.5% ± 2.97% (mean ± SD) and 3.6% ± 1.78%, respectively over the first week after treatment (Figure S6).

To further assess *in vivo* transduced CAR-T cells from peripheral blood, we used a panel of markers that included CD3, CD4, CD8, CD44, CD62L, and CD127 (Figure 3). A gating strategy for the use of these markers to define T cell immunophenotypes has been previously described,[21,22] and an example of our implementation is illustrated in Figure S5 and Table S5. At both timepoints tested (week 5 and week 8), we saw that $CD8^+$ CAR-T cells were more prevalent than $CD4^+$ CAR-T cells, and displayed mainly effector ($CD44^{high}$, $CD62L^{low}$, $CD127^{low}$) or effector memory ($CD44^{high}$, $CD62L^{low}$, $CD127^{high}$) phenotypes. Interestingly, these ID3 CAR-T cells proliferated sooner, and to a greater abundance than the FMC63 CAR-T cells, which did not become prominent until week 8. A small (<1%) but measurable population of GFP-expressing $CD4^+$ $FOXP3^+$ regulator T cells was also observed at both timepoints. We conducted quantitative polymerase chain reaction (qPCR) (Taqman) analysis to test for the presence of the CD19CAR transgene in additional tissues obtained 2 or 6 weeks after infusing mice with either of two different doses (2 × 10^7 or 2 × 10^6 IU) of the 1D3-CD19CAR-GFP virus. For the following experiments, the number of mice per treatment group was seven (n = 7). In Figure 3, error bars represent the SD away from the calculated mean of each treatment group. From peripheral blood mononuclear cell (PBMC) and spleen samples from treated mice we isolated DNA from three sorted cell populations: a T cell (CD3+) population, a B cell (CD20+) population, and an NK/NK-T and macrophage (CD335+/CD11b+) population. We also isolated DNA from lung, ovary, bone marrow, and liver from these mice. At 6 weeks, mice treated with 2 × 10^6 IU of virus showed

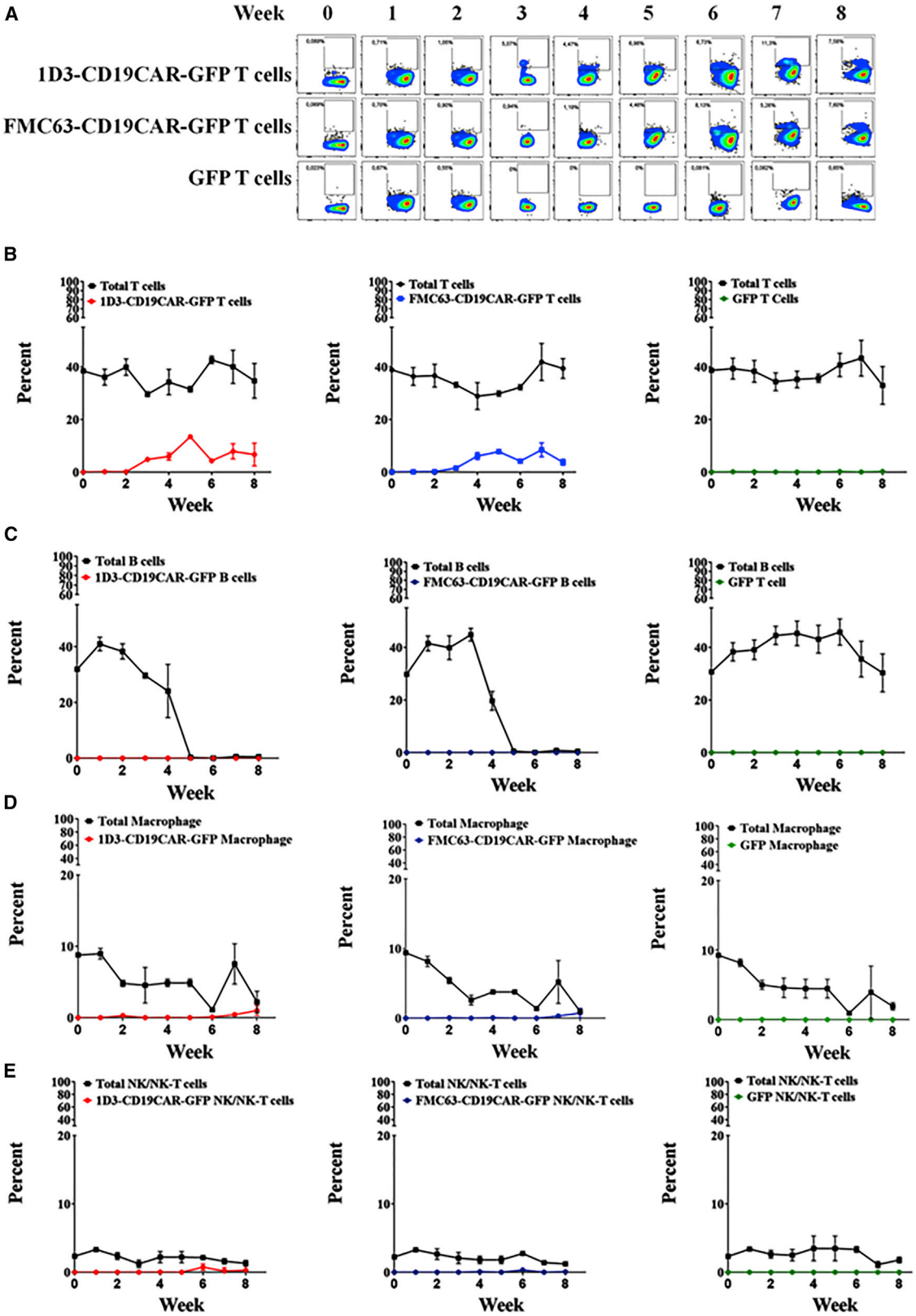

(legend on next page)

a relative quantity of 132.7 ± 27.8 in PBMC-derived $CD3^+$ T cells and 131.0 ± 35.4 in spleen-derived $CD3^+$ T cells, while mice treated with 2×10^7 IU of virus showed a relative quantity of 129.9 ± 34.8 in PBMC-derived $CD3^+$ T cells and 147.1 ± 41.4 in spleen isolated $CD3^+$ T cells. Interestingly, at the earlier 2-week time point, qPCR analysis identified transduced T cells from PBMC and spleen in two of the six mice that were treated with the higher dose of 2×10^7 IU of virus, suggesting that higher T cell transduction can promote the earlier appearance of a sizable transduced T cell population, although only sporadically. None of the off-target cell types or tissues were qPCR positive for the transgene at any of the doses or timepoints (Figure 3).

DISCUSSION

There have been no previously published reports of FMC63 cross-reactivity, or that FMC63 is human specific. Zola et al.[19] initially characterized the FMC63 antibody as a mouse-human chimera with FMC63 mouse sequences for the VDJ (heavy) and VJ (light) chains with a human C region gene of IgG1, which was then tested its ability to bind human CD19 compared with normal FMC63. Pietersz et al.[23] compared the mouse/human chimera FMC63 scFv for its ability to reduce human B cell tumors by 30% in scid/scid mice and found it similar to the mouse FMC63. Initial construction of the single-chain Fv (scFv) of FMC63[19] tested the scFv only against human cell lines. Construction of an anti-CD19 CAR using this scFv[24] tested specifically against human PBMCs. Evolution of the anti-CD19 CAR designs[25,26] tested against human CD19 tumors (NALM cell lines) but not against mouse cell lines. Evaluation of the chimeric antigen receptor-modified T cells[27] tested against human cell lines and patient samples. None of these tested the effect of FMC63 against mouse CD19. The region of the FMC63 epitope (amino acids 155–172[28]) has 75% amino acid identity and 83% amino acid similarity in human and mouse, and structural prediction shows conserved conformation of this region (Figure S7).

Interestingly, murine T cells have previously been demonstrated to have lower transduction efficiencies, compared with human T cells and compared with other murine cell types,[29–32] when transduced with HIV-1-based lentiviral vectors. The viral vector system we describe here avoids some of the known barriers of murine T cells. The entry block is avoided by the use of vesicular stomatitis virus G protein (VSV-G) pseudotyped virus. Reduced Tat activation is avoided entirely by our use of a Tat-independent transfer vector with a chimeric Rous sarcoma virus long terminal repeat (LTR). Reduced LTR promoter activity is compensated by the use of an internal EF1α promoter driving the transgene. Some reduction in lentiviral integration may still be expected in murine T cells due to inefficient nuclear import of the pre-integration complex.[31] Empirically, however, we find that while our lentiviral vectors transduce murine T cells less efficiently than they transduce human T cells (Figures S2), the level of transduction of murine T cells *in vitro* and *in vivo* is sufficient.

Quantitative PCR analysis at weeks 2 and 6 post initial injection, of T cells (CD3), B cells (CD20), NK/NK-T cells (CD335 and CD11b), as well as liver, lung, ovaries, and bone marrow tissue, showed that only the T cells had detectable CAR transgene. We did not look at the *in vivo* transduction of progenitor/stem cell types like $CD34^+$ hematopoietic stem and progenitor cells or endothelial/vascular cell types. We expect that transduction events at our administered doses are below the limit of our detection, and that the transduction of the T cells are only detectable due to antigen-driven CAR-T cell expansion. Indeed, only in the higher delivered viral dose do we see any CAR transgene in the PBMC and spleen CD3+ T cells at the 2-week time point (Figure 3). Previous studies have reported transduction of hepatocytes by VSV-G pseudotyped lentiviral particles[33,34] when used in other settings. The substantially lower viral doses (2.04×10^7 IU and 2.04×10^6 IU per mouse) used in our study do not yield detectable levels of CAR transgene in other tissues. We would expect that B cells, NK/NK-T cells, and macrophages express low levels of low density lipoprotein receptor (LDL-R) and thus the transduction of these cells by VSV-G lentivirus *in vivo* would be expected to be low[35] in accordance with our lack of CAR transgene detection in these cells. However, given that other LDL-R bystander cell populations will act as viral sinks, and given that VSV-G lentiviruses are inactivated by human complement,[36] optimal dosing regimens will need to be defined empirically.

Further implications to the transduction of bystander cells are unique to the setting of anti-CD19 CAR-T therapy. For example, expression of the CAR transgene in malignant B cells by inadvertent transduction of tumor blasts is potentially problematic, because the CAR can bind CD19 antigen on the same cell and block engagement by cytolytic CAR-T cells. This is a known but rare mechanism of relapse in conventional *ex vivo* protocols.[37] Another consideration is that, while receptor transgene expression in $CD8^+$ cytolytic T cells and $CD4^+$ helper T cells is desirable,[38] expression in regulatory T cells may have a non-negligible inhibitory effect on CAR-T cell immunoreactivity over time. Utilizing modified promoters that drive CAR transgene expression in effector but not regulatory T cells is one strategy for overcoming this potential problem.

Figure 2. The abundance of immune cell subsets in treated mice over time, as a percentage of total PBMCs

C57BL/6 wild-type mice were treated with a single intravenous injection of lentivirus ($3.6–4.0 \times 10^6$ IU in 200 μL of PBS), to deliver either the 1D3-CD19CAR-GFP CAR, FMC63-CD19CAR, or control (GFP only). N equals eight mice per group and error bars represent the standard deviation (SD) from the mean value reported for each group. T cells, but not other immune cell subsets tested, show a substantial transduced cell population. (A) Representative flowgrams showing increasing GFP-positive T cells in PBMCs of treated mice, over time. The x axis of the flowgrams is CD3 positivity and GFP positivity on the y axis. (B–E). (B) Total T cells versus 1D3-, FMC63-CD19CAR, and GFP-transduced T cells ($CD3^+$, $CD90.2^+$ T cells). (C) Total B cells versus 1D3-, FMC63-CD19CAR, and GFP-transduced B cells ($CD20^+$, $CD45R/B220^+$ B cells). (D) Total macrophage versus 1D3-, FMC63-CD19CAR, and GFP-transduced macrophage ($CD11b^+$ macrophage and other non-T cells). (E) Total NK/NK-T cells versus 1D3-, FMC63-CD19CAR, and GFP-transduced NK/NK-T cells ($CD335^+$ NK/NKT cells). Flow gating strategy outlined in Figure S4 and data in Table S3 and S4.

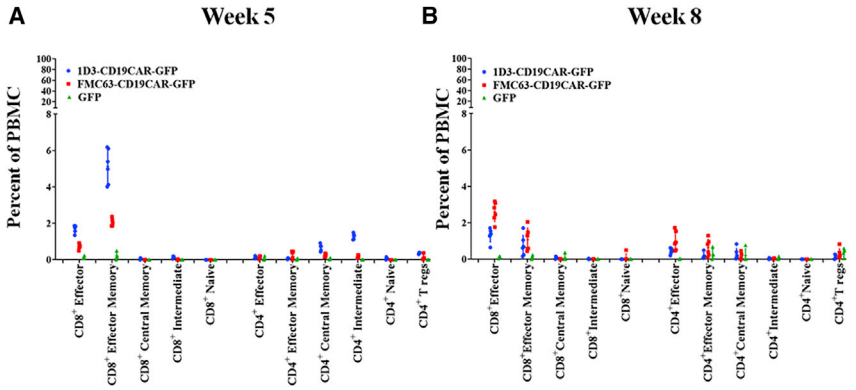

Figure 3. Immunophenotyping of 1D3-CD19CAR-GFP (blue, circle), FMC63-CD19CAR-GFP (red, square), or control (GFP only, green, triangle) transduced T cells in peripheral blood of treated mice

Values shown are the percentage of total $CD3^+$, $CD90.2^+$ T cells represented by each subtype (effector = $CD44^{high}$, $CD62L^{low}$ $CD127^{low}$; effector memory = $CD44^{high}$, $CD62L^{low}$ $CD127^{high}$; central memory = $CD44^{high}$, $CD62L^{high}$ $CD127^{high}$; intermediate phenotype = $CD44^{high}$ $CD62L^{high}$ $CD127^{low}$; naive = $CD44^{low}$, $CD62L^{high}$ $CD127^{high}$; regulatory = $CD4^+FOXP3^+$). N equals eight mice per group and error bars represent the SD from the mean value reported for each group. (A) At week 5, the 1D3-CD19CAR-GFP T cells were predominantly $CD8^+$ effector memory T cells (5.1% ± 0.9% of total $CD3^+$ T cells), effector T cells (1.7% ± 0.2% of total $CD3^+$ T cells), and $CD4^+$ intermediate T cells (1.3% ± 0.2% of total $CD3^+$ T cells). At week 5, the majority of FMC63-CD19CAR-GFP T cells were $CD8^+$ effector memory T cells (2.0% ± 0.2% of total $CD3^+$ T cells) and effector T cells (0.7% ± 0.1% of total $CD3^+$ T cells). (B) At week 8, the majority of 1D3-CD19CAR-GFP T cells were effector memory T cells (0.7% ± 0.6% of total $CD3^+$ T cells) and $CD8^+$ effector T cells (1.3% ± 0.4% of total $CD3^+$ T cells). The majority of FMC63-CD19CAR-GFP T cells at week 8 were $CD8^+$ effector memory T cells (2.60% ± 0.538% of total $CD3^+$ T cells) and effector T cells (1.1% ± 0.6% of total $CD3^+$ T cells). GFP-expressing $CD4^+$ $FOXP3^+$ regulator T cells were present at both time points but comprised a small percentage (<1%) of total T cells. Flow gating strategy outlined in Figure S5 and data in Table S5.

Insertional mutagenesis of integrating viral vectors led to highly regrettable negative outcomes in early gene therapy trials and severe setbacks to the gene therapy field.[39–44] All of these clinical trials involved *ex vivo* gene transfer to hematopoietic stem cells using first-generation gamma-retroviral vectors. Retrospective analysis has shown that the mechanism of leukemogenesis was oncogene overexpression driven by integration, in the vicinity of oncogenes, of viral vectors bearing strong promoters in their LTRs. The advent of self-inactivating lentiviral vectors with transgene expression driven by mammalian not viral LTR promoters (as used in the present study) have mitigated oncogenic risk[45,46] are now routinely used in different disease settings without incident, and no detrimental effects of insertional mutagenesis have been reported from any CAR-T clinical trial using retroviral vectors to date. Still, before clinical testing of *in vivo* CAR-T transduction could be considered, the risk of insertional mutagenesis must be fully mitigated.

The use of HIV-based lentivirus for gene transfer also raises concern about the theoretical risk of transmission of replication competent lentivirus (RCL). We use a modified second-generation lentiviral vector system with the minimal viral components included in the third-generation system split across three plasmids instead of four. These alterations abolish the potential for recombination events that can lead to formation of RCL in target cells. Testing of hundreds of cell therapy products generated with third-generation vectors as well as screening clinical trial participants after infusion of cell product failed to detect RCL,[47,48] demonstrating the safety of lentiviral gene therapy in this regard.

Clinical CAR-T protocols and other clinical IEC protocols typically include lymphodepleting chemotherapy with cyclophosphamide and/or fludarabine as preconditioning. While it would not be productive to perform complete lymphoablation prior to a viral infusion protocol (because endogenous T cells must be present for virus to transduce), mild preconditioning may be beneficial, if depletion leaves enough endogenous T cells in circulation to support viral transduction and conversion to CAR-Ts, while at the same time providing a niche for robust CAR-T expansion and engraftment.[38] This could be further tested, but it may be unnecessary given our results show full ablation of endogenous B cells after lentiviral infusion (Figure 2C) without any preconditioning lymphodepletion.

In summary, anti-CD19 CAR-T therapy for B cell malignancies has shown clinical success, but a major limitation is the logistical complexity and high cost of manufacturing autologous cell products. This has led to increasing interest in industry and academia in universal (non-personalized) strategies. Here we report that intravenous infusion of replication-incompetent VSV-G-pseudotyped lentiviral particles carrying an anti-CD19 CAR transgene with either an FMC63 or ID3 anti-CD19 binding domain can effectively transduce murine T cells, leading to CAR-T proliferation and subsequent CAR-T-mediated B cell aplasia. Our study supports the notion that CAR-T cells expanded *in vivo* could be effective against B cell malignancies, which requires further study. This observation also supports this modality as a potential universal CAR-T intervention that could have clinical relevance if further engineering is able to overcome the safety concerns and other limitations of systemic viral gene therapy.

MATERIALS AND METHODS

Media

RPMI-1640 supplemented medium (sRPMI-1640) consisted of 2 mM GlutaMAX (Invitrogen, 35050-061), 1 mM MEM non-essential amino acid (Invitrogen, 11140-050), 1 mM sodium pyruvate (Invitrogen, 11360-070), 10 mM HEPES (Invitrogen, 15630-808), 100 U/mL penicillin-streptomycin (Invitrogen, 15140-122), MycoZap prophylactic (Lonza, VZA-2031), 0.05 mM 2-beta mercaptoethanol (Sigma, 60-42-2, 2-βME added to medium for murine cell cultures only), and 10% heat-inactivated fetal bovine serum (Invitrogen, 12484-028). For

expansion cultures, IL-2 (StemCell, 78036.3 or Miltenyi Biotech, 130-097-745) was added to the sRPMI-1640 medium. Cells were cultured in sRPMI-1640 with a final IL-2 concentration of 300 IU/mL, unless otherwise stated. Fluorescence-activated cell sorting (FACS) medium consisted of 1× D-PBS (Sigma, 59331C) with 2% HI-FCS. In-house MACS (Magnetic-activated cell sorting) separation buffer consisted of D-PBS with 2 mM EDTA (Thermo Fisher, 15575020) and 2% HI-FBS.

Production of lentiviral gene transfer vectors

Our lentivector system is a modified second-generation system that uses three separate plasmids to split the lentiviral genome as previously described.[49,50] The system comprises a packaging plasmid encoding gag, pol, and rev (Figure S8); a VSV-G envelope-expressing plasmid (Figure S9); and a transfer plasmid encoding the transgene (Figure S10). Biosafety of the second-generation design was improved by removal of tat from the packaging plasmid with the concurrent replacement of the transfer vector 5′ LTR with chimeric sequence for Tat-independent expression and a self-inactivating modified 3′ LTR.[51] These modifications serve to prevent the formation of replication-competent virus. Synthetic transgene sequences encoding (1) GFP, (2) FMC63-CD19CAR-2A-GFP, and (3) 1D3-CD19CAR-2A-GFP were manufactured (ATUM) containing the FMC63 (anti-human) or 1D3 (anti-mouse) anti-CD19 scFv with human co-stimulatory 4-1BB activation domains as a CAR, subcloned into the transfer plasmid and verified by Sanger sequencing (Genewiz). Envelope (VSV-G) and packaging (GagPolRev) plasmids were also manufactured (ATUM). To manufacture virus particles, envelope, packaging, and transfer plasmids were co-transfected into the packaging cell line HEK-293T (clone 17; ATCC) using TransIT-LT1 (Mirus, MIR2305). Medium containing the lentivirus was collected after transfection, filtered, and then ultracentrifuged at 25,000 rpm or 106,750 × *g*, for 90 min at 4°C (Optima XE-90, Beckman-Coulter with SW 32 Ti swinging bucket rotor) to pellet the virus. Viral pellets were resuspended in 1× D-PBS and aliquoted for long-term storage at −80C. Functional viral titers were established by infection of K562 cells (ATCC) and EL4 cells (ATCC) determined by transducing 5×10^4 EL4 or K562 cells (ATCC) with 1, 2, 4, 8, 16, or 32 μL of concentrated viral supernatant. Performed in duplicate, cells were suspended in a final volume of 500 μL of sRPMI-1640 medium, in the 24-well format. Cells were then incubated for 72 h, before being washed, centrifuged, and resuspended in FACS medium. Acquisition was performed on the BD LSRFortessa cell analyzer, and analyzed using FlowJo and GraphPad Prism software version 8.0.0 for Windows (GraphPad Software, CA, USA) (Figure S1).

Sample acquisition and storage

Human PBMCs were isolated by Ficoll gradient purification as per manufactures protocol (Ficoll, GE-17-1440, GE Healthcare) from human peripheral blood leukapheresis pack (StemCell). Between 100 and 150 μL of C57BL/6 mouse blood was collected in lithium heparin capillary tubes via tail vein blood sampling before treatment and then every week post treatment for 8 weeks. The blood samples were diluted with 1–1.5 mL of cold RPMI, which was overlayed with 4 mL of Ficoll, and C57BL/6 mouse PBMCs were isolated following the manufacturer's protocol. C57BL/6 mouse PBMCs were isolated and analyzed within 24 h of isolation. PBMCs were resuspended in sRPMI-1640 at a concentration of 1×10^6 cells/mL, placed into a T25 culture flask (156367, Thermo Fisher), and rested overnight in the cell incubator at 37°C with 5% CO_2 airflow before being used in any analysis. Human PBMCs and C57BL/6 mouse PBMCs not immediately used in any experiments were stored down by resuspending cells in freezing medium (HI-FBS with 10% DMSO, Fisher Scientific, BP231-100) in aliquots of $5–10 \times 10^6$ cells/mL and frozen down to −80°C at a speed of 1°C/min prior to storage in liquid nitrogen.

The C57BL/6 mouse splenocytes used in the *in vitro* assays were acquired from naive or untreated C57BL/6 mice, aged 4–8 weeks old. All C57BL/6 mice were, however, processed the same way by first manually dissociating the spleens and filtering them through a 70-μm cell strainer (Corning, CLS431751) into a 50-mL falcon tube, and centrifuged at 400 × *g* for 10 min (Eppendorf Centrifuge 5810R, rotor A-4-62) at room temperature to pellet the cells. The splenocytes samples were resuspended in 5 mL of ammonium-chloride-potassium (ACK) lysing buffer (Thermo Fisher), before incubating the cells on ice for no longer than 4 min before 10 mL of sRPMI-1640 medium was added to the cells to neutralize the ACK buffer and wash the splenocytes. The splenocytes were then centrifuged at 400 × *g* for 10 min (Eppendorf Centrifuge 5810R, rotor A-4-62) at room temperature, the supernatant was removed, and the splenocytes were washed again before being resuspended in sRPMI-1640 medium and cell numbers obtained using the Countess automated cell counter (Thermo Fisher). Splenocytes were stored down by resuspending cells in freezing medium (HI-FBS with 10% DMSO, Fisher Scientific, BP231-100) in aliquots of $5–10 \times 10^6$ cells/mL and frozen down to −80°C at a speed of 1°C/min prior to storage in liquid nitrogen.

The acquired bone marrow, ovaries, lung, and liver tissues were manually dissociated and filtered through a 70-μm cell strainer (Corning, CLS431751) into a 50-mL falcon tube. Samples were then washed with D-PBS and centrifuged at 400 × *g* for 10 min (Eppendorf Centrifuge 5810R, rotor A-4-62) at room temperature to pellet the cells. The cells were counted and stored in RNA later (AM7021, Thermo Fisher) following the manufactures protocols. DNA was extracted from these samples using the DNeasy Blood and Tissue kit (Qiagen, 69,504) following the manufacturer's protocol.

In vitro 1D3-and FMC63-CD19CAR-GFP modified T cell expansion and testing using C57BL/6 mouse splenocytes

C57BL/6 mouse splenocytes were removed from liquid nitrogen storage, thawed, and resuspended in sRPMI-1640 with 300 IU/mL of IL-2, and 30 ng/mL of CD3 (clone 145-2C11, 100314, BioLegend) and 30 ng/mL CD28 (clone 37.51, 102112, BioLegend) antibodies, at a concentration of 1×10^6 cells/mL. The splenocytes were then treated with 1D3-, FMC63-CD19CAR-GFP, or GFP-only viral supernatant at an MOI of 5 (calculated based on titration data) and incubated for 72 h. Following transduction, cells were washed by

resuspending the cells in sRPMI-1640, centrifuging them at 400 × *g* for 10 min at room temperature (Eppendorf Centrifuge 5810R, rotor A-4-62), removing the supernatant, and repeating the process a further two times. The cells were resuspended in sRPMI-1640 medium containing 300 IU/mL of IL-2 at a concentration of 2.5×10^5 cells/mL, with 1 mL being aliquoted per well, in the six-well culture plate format. Irradiated autologous murine splenocytes (50 Gy) were resuspended in sRPMI-1640 medium containing 300 IU/mL of IL-2 at a concentration of 2.5×10^7/mL and 1 mL was added to the transduced splenocytes giving a final ratio of 1:100 transduced splenocytes to irradiated splenocytes. Every third day, 1 mL of the culture medium was removed and 1 mL of fresh sRPMI-1640 medium with 600 IU/mL of IL-2 was added (giving a final concentration of 300 IU/mL IL-2). On days 0, 14, 28, and 63, the cells were counted using the Countess automated cell counter (Thermo Fisher) and an aliquot of 3×10^4 cells was stained with fluorescent labeled antibodies and analyzed using flow cytometry (Figures 1A and 1B).

In a 96-well plate format with a final volume of 200 μL (sRPMI-1640), 1×10^5 1D3-, FMC63-CD19CAR, or GFP-transduced T cells from day 63 of the expansion were co-cultured for 5 h with 1×10^5 B cells isolated from another sample of C57BL/6 mouse splenocytes, using the Miltenyi MACS mouse CD19 B cell isolation beads, following the manufacturer's protocol and using an MACS separation buffer made in house. At the end of the co-culture, the cells were stained with fluorescent labeled antibodies and analyzed using flow cytometry (Figure 1C). Cells were washed with 500 μL of D-PBS and centrifuged at 400 × *g* for 10 min at room temperature (Eppendorf Centrifuge 5810R, rotor A-4-62). The supernatant was removed and the cell pellet resuspended in 50 μL of D-PBS before being stained with CD20-PE (clone A1SB12, 12-0201-82, eBioscience), CD3-efluor 450 (clone 17A2, 48-0032-82, eBioscience), and the non-viable cell marker, Fixable Viability Stain 780 (FVS780) (565,388, BD Biosciences). Cells and antibodies were incubated at 4°C for 30 min, then washed by adding 2 mL of FACS medium to each tube and centrifuging for 10 min at 400 × *g* at 4°C followed by removal of the supernatant before resuspension in 500 μL of cold FACS medium. Flow cytometry acquisition was performed using the BD LSRFortessa cell analyzer with BD FACSDiva software. The analysis was performed using FlowJo software, version 10 for Windows, and GraphPad Prism software version 8.0.0 for Windows (GraphPad Software, CA, USA) (Figure S3 and Table S1).

In vitro 1D3-and FMC63-CD19CAR-GFP modified mouse T cells co-culture with A20 cells

C57BL/6 mouse splenocytes were transduced with 1D3-, FMC63-CD19CAR-GFP, or GFP-only viral supernatant, sorted, and expanded as previously mentioned. The murine, CD19 expressing A20 cell line (ATCC) was used as the target cells in a co-culture with the sorted and expanded 1D3-, FMC63-CD19CAR-GFP, or GFP-only expressing murine T cells. In order to verify the ability for both the 1D3-and FMC63-CD19CAR to target the mouse CD19 antigen, the A20 cells were incubated with 10, 1, 0.1, 0.001, or 0 μg/mL of either the 1D3-CD19-blocking antibody (152402, BioLegend) or the FMC63-CD19-blocking antibody (NBP2-52716, Novus Biologicals). In the 96-well plate format with a final volume of 200 μL (sRPMI-1640), the A20 cells were then co-cultured with the 1D3-, FMC63-CD19CAR-GFP, or GFP-only expressing murine T cells at an effector to target ratio of 4:1(2×10^5:5×10^4) for 4 h. Cells were then washed and stained with CD20-PE, CD3-efluor 450, and the non-viable cell marker, Fixable Viability Stain 780 (FVS780) as previously described (Figure S3 and Table S2). Flow cytometry acquisition was performed using the BD LSRFortessa cell analyzer with BD FACSDiva software. The analysis was performed using FlowJo software, version 10 for Windows, and GraphPad Prism software version 8.0.0 for Windows (GraphPad Software, CA, USA) (Figure 1D).

In vivo testing

All animal experiments were assessed and approved by the University of British Columbia's Animal Care Committee under ethics certificate #A17-0107. For the *in vivo* testing, C57BL/6 mice, aged 4 to 8 weeks old, were obtained from the BC Cancer Research Centre's Animal Resource Centre. The experimental mice received one tail vein infusion on day 1, which involved the intravenous injection of 200 μL of D-PBS containing 3.6–4 × 10^6 total IU of either 1D3, FMC63-CD19CAR-GFP, or GFP only. For subsequent dose-response *in vivo* experiments, mice received an intravenous injection of 200 μL of D-PBS containing either 2.04×10^6 or 2.04×10^7 total IU of 1D3-CD19CAR-GFP. Mice were monitored closely for the first 72 h, and then once a day until the experimental endpoint. The mice were also weighed periodically and blood collected in lithium heparin capillary tubes via tail vein sampling as previously described. At the experimental endpoint, the mice were humanly euthanized and spleen and blood tissue collected and processed as previously described. The cells were stained with fluorescent labeled antibodies and analyzed using flow cytometry (Figures 2 and 3). DNA from the cells of the various tissues was collected and the samples analyzed for CD19CAR-GFP possession using qPCR (Figure 4).

For flow cytometry acquisition and analysis, 4×10^5 cells were stained with CD3-efluor 450 (clone 17A2, 48-0032-82, eBioscience), CD90.2-AF700 (clone 30-H12, 105319, BioLegend), CD20-PE (clone A1SB12, 12-0201-82, eBioscience), CD45R/B220-APC-CY7 (clone RA3-6B2, 103223, BioLegend), CD335-APC (clone 29A1.4, 137608, BioLegend), and CD11B-BV605 (clone M1/79, 101237, BioLegend) conjugated flow antibodies. Cells and antibodies were incubated at 4°C for 30 min, then washed by adding 2 mL of FACS medium to each tube and centrifuging for 10 min at 400 × *g* at 4°C, discarding the supernatant before resuspension in 500 μL of cold FACS medium. Acquisition was performed on the BD LSRFortessa cell analyzer, and analysis was performed using FlowJo and GraphPad Prism software version 8.0.0 for Windows (GraphPad Software, CA, USA) (Figure S4; Table S3 and S4).

In the immunophenotyping analysis (Figure 3), up to 5×10^4 cells were stained with CD3-efluor 450 (clone 17A2, 48-0032-82, eBioscience), CD4-PE (clone GK1.5, 100408, BioLegend), CD8-BUV395 (clone QA17A07, 155006, BioLegend), CD44-alexa fluor 700 (clone

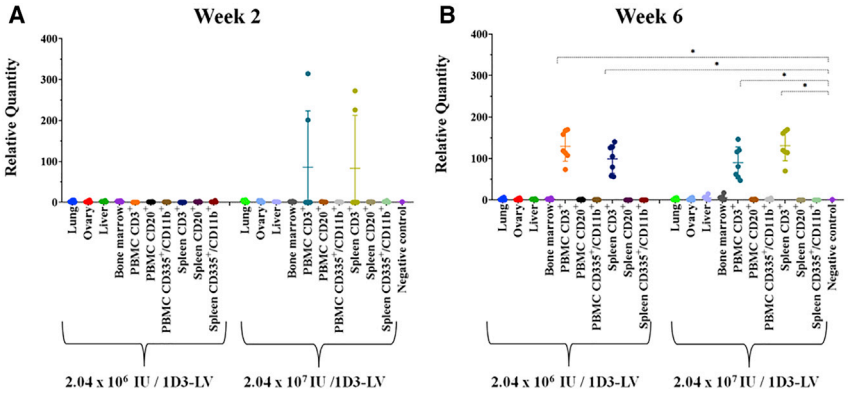

Figure 4. Quantitative PCR analysis of transgene positivity

DNA from $CD3^+$, $CD20^+$, and $CD355^+/11b^+$ cells, sorted from PBMC and spleen samples and from liver, lung, bone marrow, and the ovaries was obtained from female C57BL/6 mice. N equals seven mice per group and the error bars represent the SD from the mean value reported for each group (A). Two weeks and (Figure 3B) 6 weeks after being treated with 2.04×10^6 or 2.04×10^7 IU of the 1D3-CD19CAR lentivirus, respectively. The 1D3-CD19CAR-GFP transgenes were prominent only in the $CD3^+$ T cell populations isolated from both PBMC and spleens 6 weeks post 1D3-CD19CAR-LV treatment (B). Orange 132.7 ± 27.77, dark blue 131.0 ± 35.42, cyan 129.9 ± 34.75, and mustard 147.1 ± 41.42. Relative quantity was calculated using the ΔΔCT calculation using the murine reference gene β-actin and unmodified C57BL/6 spleen cells as the reference control. We also see evidence of CD19CAR-T possession at week 2, in $CD3^+$ T cells isolated from the spleen and PBMCs of two mice that received 2.04×10^7 IU of the 1D3-CD19CAR-LV (A; cyan and mustard). (A) ANOVA ***$p < 0.001$, (B) ANOVA***$p < 0.001$. Using Dunnett's post hoc analysis, comparing PBMC and spleen T cells, 6 weeks after treatment with 2.04×10^6 of the 1D3-CD19CAR-LV with the negative control, *$p > 0.015$.

IM7, 103026, BioLegend), CD62L-PerCP-CY5.5 (clone MEL-14, 104432, BioLegend), CD127-APC-CY7 (clone A7R34, 135040, BioLegend), CD25-PE-CF594 (clone PC61, 562694, BD Biosciences), and FOXP3-APC (clone FJK-16s, 563786, BD Biosciences) and incubated at 4°C for 30 min, as previously mentioned. The cells were then fixed by incubating the cells in up to 200 μL of fixation buffer (420801, BioLegend) at 4°C for 30 min. The cells were than washed by adding 2 mL of FACS medium and centrifuging for 10 min at 400 × *g* at 4°C, and resuspended in 1× Intracellular Staining Perm Wash Buffer (10× stock solution, diluted to 1× with ddH_2O, 420801, BioLegend) at 4°C for 30 min, before being stained with FOXP3-APC (at 4°C for 30 min). Again cells were washed by adding 2 mL of FACS medium and centrifuging for 10 min at 400 × *g* at 4°C, discarding the supernatant before resuspension in 500 μL of cold FACS medium. Acquisition was performed on the BD LSRFortessa cell analyzer, and analyzed using FlowJo and GraphPad Prism software version 8.0.0 for Windows (GraphPad Software, CA, USA) (Figure S5 and Table S5). For all flow analyzes, we used the CD20-PE antibody as a B cell marker in place of a CD19 antibody (Figures 1 and 2) to avoid any possible interference between anti-CD19 antibody and anti-CD19 CARs in these mixed cell populations.

Quantitative PCR of DNA isolated from mouse tissues

Spleens and PBMC from 2 to 6 weeks post 1D3-CD19CAR-LV treatment were sorted into CD3-, CD20-, and CD335/CD11b-expressing cell types using BD FACSAria and BD FACSDiva software (Figure S4). DNA was then extracted from the spleen and PBMC sorted cell subtypes, along with the DNA from liver, ovaries, lung, and bone marrow tissues (stored in RNA later) collected using the DNeasy Blood and Tissue kit (Qiagen, 69504) following the manufacturer's protocol. The DNA concentrations were read using NanoDrop 8000 Spectrophotometer (ND-8000-GL, Thermo Fisher) by following the manufactures protocol. The DNA concentration was normalized to a concentration of 19–21 ng/μL. The presence of the CD19CAR gene was detected using a Taqman primer probe set that amplifies DNA from the co-stimulatory and activation domains of the 1D3-CD19CAR-T transgene. For every 2 μL of template DNA, 0.5 μL of the CD19CAR[44] and murine β-actin Taqman assay sets (4352341, Thermo Fisher) and 5 μL of Taqman Fast Advanced 364 Master Mix (4444557, Invitrogen) were used, brought to a final volume of 10 μL with ultrapure water (10977023, Invitrogen). Thermocycling was done using the QuantStudio 6 Flex System, in the 384-well format, using the comparative Ct (ΔΔCt) setup. Thermocycling conditions were one cycle at 50°C for 2 min, 1 cycle at 95°C for 2 min, then 95°C for 2 s and 60°C for 20 s for 40 cycles, capturing data at the end of every cycle. For the analysis, the mouse β-actin gene was used as the endogenous control and an *in vitro* transduced spleen sample, positive for 1D3-CD19CAR-GFP possession, was used as a positive control. Spleen cells from an untreated mouse were used as the reference control for the ΔΔCT calculation required to obtain a relative quantity.

Thermocycling was done using the QuantStudio 6 Flex System, in the 384-well format, using the comparative Ct (ΔΔCt) setup. Thermocycling conditions were one cycle at 50°C for 2 min, 1 cycle at 95°C for 2 min, then 95°C for 3 s and 60°C for 30 s for 40 cycles, capturing data at the end of every cycle. For the analysis, the mouse β-actin gene was used as the endogenous control and the $CD3^+$ PBMC and spleen from phosphate buffered saline (PBS)-treated mouse from week 1 and week 8 were used as the reference control, as these samples showed the lowest relative quantity, as they were treated with PBS.

SUPPLEMENTAL INFORMATION

Supplemental information can be found online at https://doi.org/10.1016/j.omtm.2022.05.006.

ACKNOWLEDGMENTS

This research was supported by the British Columbia Cancer Foundation, the Leon Judah Blackmore Foundation, the BioCanRx network, and the Canadian Institutes of Health Research (CIHR).

AUTHOR CONTRIBUTIONS

R.A.H., C.M.R., and E.Y. designed research. C.M.R., E.Y., L.D., C.G.M., and D.J.W. performed research. C.M.R. and S.D.B. analyzed data. All authors prepared and edited the manuscript.

DECLARATION OF INTERESTS

The authors declare no competing interests.

REFERENCES

1. Neelapu, S.S., Locke, F.L., Bartlett, N.L., Lekakis, L.J., Miklos, D.B., Jacobson, C.A., Braunschweig, I., Oluwole, O.O., Siddiqi, T., Lin, Y., et al. (2017). Axicabtagene ciloleucel CAR T-cell therapy in refractory large B-Cell lymphoma. N. Engl. J. Med. *377*, 2531–2544.
2. Maude, S.L., Laetsch, T.W., Buechner, J., Rives, S., Boyer, M., Bittencourt, H., Bader, P., Verneris, M.R., Stefanski, H.E., Myers, G.D., et al. (2018). Tisagenlecleucel in children and young adults with B-cell lymphoblastic leukemia. N. Engl. J. Med. *378*, 439–448.
3. Park JH, Rivière I, Gonen M, Wang X, Sénéchal B, Curran KJ, Sauter C, Wang Y, Santomasso B, Mead E, et al. Long-term follow-up of CD19 CAR therapy in acute lymphoblastic leukemia. N. Engl. J. Med. 2018 Feb 1;378(5):449–459.
4. Hay KA, Gauthier J, Hirayama AV, Voutsinas JM, Wu Q, Li D, Gooley TA, Cherian S, Chen X, Pender BS, et al. Factors associated with durable EFS in adult B-cell ALL patients achieving MRD-negative CR after CD19 CAR T-cell therapy. Blood. 2019 Apr 11;133(15):1652–1663.
5. Hirayama, A.V., Gauthier, J., Hay, K.A., Voutsinas, J.M., Wu, Q., Pender, B.S., Hawkins, R.M., Vakil, A., Steinmetz, R.N., Riddell, S.R., et al. (2019). High rate of durable complete remission in follicular lymphoma after CD19 CAR-T cell immunotherapy. Blood *134*, 636–640. http://www.ncbi.nlm.nih.gov/pubmed/31648294.
6. Schuster, S.J., Svoboda, J., Chong, E.A., Nasta, S.D., Mato, A.R., Anak, Ö., Brogdon, J.L., Pruteanu-Malinici, I., Bhoj, V., Landsburg, D., et al. (2017). Chimeric antigen receptor T Cells in refractory B-Cell lymphomas. N. Engl. J. Med. *377*, 2545–2554.
7. Grigor, E.J.M., Fergusson, D., Kekre, N., Montroy, J., Atkins, H., Seftel, M.D., et al. (2019). Risks and benefits of chimeric antigen receptor T-cell (CAR-T) therapy in cancer: a systematic review and meta-analysis, *33* (Transfusion Medicine Reviews), pp. 98–110.
8. Sommer, C., Boldajipour, B., Kuo, T.C., Bentley, T., Sutton, J., Chen, A., Geng, T., Dong, H., Galetto, R., Valton, J., et al. (2019). Preclinical evaluation of allogeneic CAR T cells targeting BCMA for the treatment of multiple myeloma. Mol. Ther. *27*, 1126–1138. http://www.ncbi.nlm.nih.gov/pubmed/31005597.
9. Qasim, W., Zhan, H., Samarasinghe, S., Adams, S., Amrolia, P., Stafford, S., Butler, K., Rivat, C., Wright, G., Somana, K., et al. (2017). Molecular remission of infant B-ALL after infusion of universal TALEN gene-edited CAR T cells. Sci. Transl. Med. *9*. https://doi.org/10.1126/scitranslmed.aaj2013. http://www.ncbi.nlm.nih.gov/pubmed/28123068.
10. Brudno, J.N., Somerville, R.P.T., Shi, V., Rose, J.J., Halverson, D.C., Fowler, D.H., Gea-Banacloche, J.C., Pavletic, S.Z., Hickstein, D.D., Lu, T.L., et al. (2016). Allogeneic T cells that express an anti-CD19 chimeric antigen receptor induce remissions of B-cell malignancies that progress after allogeneic hematopoietic stem-cell transplantation without causing graft-versus-host disease. J. Clin. Oncol. *34*, 1112–1121. https://doi.org/10.1200/JCO.2015.64.5929. http://www.ncbi.nlm.nih.gov/pubmed/26811520.
11. Williams, B.A., Law, A.D., Routy, B., DenHollander, N., Gupta, V., Wang, X.-H., Chaboureau, A., Viswanathan, S., and Keating, A. (2017). A phase I trial of NK-92 cells for refractory hematological malignancies relapsing after autologous hematopoietic cell transplantation shows safety and evidence of efficacy. Oncotarget *8*, 89256–89268. https://doi.org/10.18632/oncotarget.19204. http://www.ncbi.nlm.nih.gov/pubmed/29179517.
12. Shukla, S., Langley, M.A., Singh, J., Edgar, J.M., Mohtashami, M., Zúñiga-Pflücker, J.C., and Zandstra, P.W. (2017). Progenitor T-cell differentiation from hematopoietic stem cells using Delta-like-4 and VCAM-1. Nat. Methods *14*, 531–538. https://doi.org/10.1038/nmeth.4258.
13. Smith, T.T., Stephan, S.B., Moffett, H.F., McKnight, L.E., Ji, W., Reiman, D., Bonagofski, E., Wohlfahrt, M.E., Pillai, S.P.S., and Stephan, M.T. (2017). In situ programming of leukaemia-specific T cells using synthetic DNA nanocarriers. Nat. Nanotechnol. *12*, 813–820. http://www.ncbi.nlm.nih.gov/pubmed/28416815.
14. Aghajanian, H., Kimura, T., Rurik, J.G., Hancock, A.S., Leibowitz, M.S., Li, L., Scholler, J., Monslow, J., Lo, A., Han, W., et al. (2019). Targeting cardiac fibrosis with engineered T cells. Nature *573*, 430–433. https://doi.org/10.1038/s41586-019-1546-z. http://www.ncbi.nlm.nih.gov/pubmed/31511695.
15. Pfeiffer, A., Thalheimer, F.B., Hartmann, S., Frank, A.M., Bender, R.R., Danisch, S., Costa, C., Wels, W.S., Modlich, U., Stripecke, R., et al. (2018). In vivo generation of human CD 19- CAR T cells results in B-cell depletion and signs of cytokine release syndrome. EMBO Mol. Med. *10*, e9158. https://doi.org/10.15252/emmm.201809158.
16. Frank, A.M., Braun, A.H., Scheib, L., Agarwal, S., Schneider, I.C., Fusil, F., Perian, S., Sahin, U., Thalheimer, F.B., Verhoeyen, E., and Buchholz, C.J. (2020). Combining T-cell-specific activation and in vivo gene delivery through CD3-targeted lentiviral vectors. Blood Adv *4*, 5702–5715. http://www.ncbi.nlm.nih.gov/pubmed/33216892.
17. Agarwal, S., Hanauer, J.D.S., Frank, A.M., Riechert, V., Thalheimer, F.B., and Buchholz, C.J. (2020). In vivo generation of CAR T cells selectively in human CD4+ lymphocytes. Mol. Ther. *28*, 1783. https://doi.org/10.1016/j.ymthe.2020.05.005. http://www.ncbi.nlm.nih.gov/pubmed/32485137.
18. Imai, C., Mihara, K., Andreansky, M., Nicholson, I.C., Pui, C.-H.H., Geiger, T.L., and Campana, D. (2004). Chimeric receptors with 4-1BB signaling capacity provoke potent cytotoxicity against acute lymphoblastic leukemia. Leukemia *18*, 676–684. http://www.ncbi.nlm.nih.gov/pubmed/14961035.
19. Nicholson, I.C., Lenton, K.A., Little, D.J., Decorso, T., Lee, F.T., Scott, A.M., Zola, H., and Hohmann, A.W. (1997). Construction and characterisation of a functional CD19 specific single chain Fv fragment for immunotherapy of B lineage leukaemia and lymphoma. Mol. Immunol. *34*, 1157–1165. http://www.ncbi.nlm.nih.gov/pubmed/9566763.
20. Kochenderfer, J.N., Yu, Z., Frasheri, D., Restifo, N.P., and Rosenberg, S.A. (2010). Adoptive transfer of syngeneic T cells transduced with a chimeric antigen receptor that recognizes murine CD19 can eradicate lymphoma and normal B cells. Blood *116*, 3875–3886. http://www.ncbi.nlm.nih.gov/pubmed/20631379.
21. Huster, K.M., Koffler, M., Stemberger, C., Schiemann, M., Wagner, H., and Busch, D.H. (2006). Unidirectional development of CD8+ central memory T cells into protective Listeria-specific effector memory T cells. Eur. J. Immunol. *36*, 1453–1464. http://www.ncbi.nlm.nih.gov/pubmed/16637009.
22. Bachmann, M.F., Wolint, P., Schwarz, K., Jäger, P., and Oxenius, A. (2005). Functional properties and lineage relationship of CD8+ T cell subsets identified by expression of IL-7 receptor alpha and CD62L. J. Immunol. *175*, 4686–4696. http://www.ncbi.nlm.nih.gov/pubmed/16177116.
23. Pietersz, G.A., Wenjun, L., Sutton, V.R., Burgess, J., McKenzie, I.F.C., Zola, H., and Trapani, J.A. (1995). In vitro and in vivo antitumor activity of a chimeric anti-CD19 antibody. Cancer Immunol. Immunother. *41*, 53–60. http://www.ncbi.nlm.nih.gov/pubmed/7543822.
24. Kochenderfer, J.N., Feldman, S.A., Zhao, Y., Xu, H., Black, M.A., Morgan, R.A., Wilson, W.H., and Rosenberg, S.A. (2009). Construction and preclinical evaluation of an anti-CD19 chimeric antigen receptor. J. Immunother. *32*, 689–702. http://www.ncbi.nlm.nih.gov/pubmed/19561539.
25. Qin, L., Lai, Y., Zhao, R., Wei, X., Weng, J., Lai, P., Li, B., Lin, S., Wang, S., Wu, Q., et al. (2017). Incorporation of a hinge domain improves the expansion of chimeric antigen receptor T cells. J. Hematol. Oncol. *10*, 68. https://doi.org/10.1186/s13045-017-0437-8. http://www.ncbi.nlm.nih.gov/pubmed/28288656.
26. Rodgers, D.T., Mazagova, M., Hampton, E.N., Cao, Y., Ramadoss, N.S., Hardy, I.R., Schulman, A., Du, J., Wang, F., Singer, O., et al. (2016). Switch-mediated activation and retargeting of CAR-T cells for B-cell malignancies. Proc. Natl. Acad. Sci. U S A *113*, E459–E468. http://www.ncbi.nlm.nih.gov/pubmed/26759369.
27. Sommermeyer, D., Hudecek, M., Kosasih, P.L., Gogishvili, T., Maloney, D.G., Turtle, C.J., and Riddell, S.R. (2016). Chimeric antigen receptor-modified T cells derived from defined CD8+ and CD4+ subsets confer superior antitumor reactivity in vivo. Leukemia *30*, 492–500. https://doi.org/10.1038/leu.2015.247. http://www.ncbi.nlm.nih.gov/pubmed/26369987.

28. Klesmith, J.R., Wu, L., Lobb, R.R., Rennert, P.D., and Hackel, B.J. (2019). Fine epitope mapping of the CD19 extracellular domain promotes design. Biochemistry *58*, 4869–4881. https://doi.org/10.1021/acs.biochem.9b00808. http://www.ncbi.nlm.nih.gov/pubmed/31702909.

29. Baumann, J.G., Unutmaz, D., Miller, M.D., Breun, S.K.J., Grill, S.M., Mirro, J., Littman, D.R., Rein, A., and KewalRamani, V.N. (2004). Murine T cells potently restrict human immunodeficiency virus infection. J. Virol. *78*, 12537–12547. https://doi.org/10.1128/jvi.78.22.12537-12547.2004.

30. Kerkar, S.P., Sanchez-Perez, L., Yang, S., Borman, Z.A., Muranski, P., Ji, Y., Chinnasamy, D., Kaiser, A.D.M., Hinrichs, C.S., Klebanoff, C.A., et al. (2011). Genetic engineering of murine CD8+ and CD4+ T cells for preclinical adoptive immunotherapy studies. J. Immunother. *34*, 343–352. http://www.ncbi.nlm.nih.gov/pubmed/21499127.

31. Tsurutani, N., Yasuda, J., Yamamoto, N., Choi, B.-I., Kadoki, M., and Iwakura, Y. (2007). Nuclear import of the preintegration complex is blocked upon infection by human immunodeficiency virus type 1 in mouse cells. J. Virol. *81*, 677–688. https://doi.org/10.1128/jvi.00870-06.

32. Delville, M., Soheili, T., Bellier, F., Durand, A., Denis, A., Lagresle-Peyrou, C., Cavazzana, M., Andre-Schmutz, I., and Six, E. (2018). A nontoxic transduction enhancer enables highly efficient lentiviral transduction of primary murine T cells and hematopoietic stem cells. Mol Ther - Methods Clin Dev. *10*, 341–347. https://doi.org/10.1016/j.omtm.2018.08.002.

33. Follenzi, A., Battaglia, M., Lombardo, A., Annoni, A., Roncarolo, M.G., and Naldini, L. (2004). Targeting lentiviral vector expression to hepatocytes limits transgene-specific immune response and establishes long-term expression of human antihemophilic factor IX in mice. Blood *103*, 3700–3709. https://doi.org/10.1182/blood-2003-09-3217. http://www.ncbi.nlm.nih.gov/pubmed/14701690.

34. Pan, D., Gunther, R., Duan, W., Wendell, S., Kaemmerer, W., Kafri, T., Verma, I.M., and Whitley, C.B. (2002). Biodistribution and toxicity studies of VSVG-pseudotyped lentiviral vector after intravenous administration in mice with the observation of in vivo transduction of bone marrow. Mol. Ther. *6*, 19–29. http://www.ncbi.nlm.nih.gov/pubmed/12095299.

35. Amirache, F., Lévy, C., Costa, C., Mangeot, P.-E., Torbett, B.E., Wang, C.X., Nègre, D., Cosset, F.-L., and Verhoeyen, E. (2014). Mystery solved: VSV-G-LVs do not allow efficient gene transfer into unstimulated T cells, B cells, and HSCs because they lack the LDL receptor. Blood *123*, 1422–1424. https://doi.org/10.1182/blood-2013-11-540641. http://www.ncbi.nlm.nih.gov/pubmed/24578496.

36. DePolo, N.J., Reed, J.D., Sheridan, P.L., Townsend, K., Sauter, S.L., Jolly, D.J., and Dubensky, T.W. (2000). VSV-G pseudotyped lentiviral vector particles produced in human cells are inactivated by human serum. Mol. Ther. *2*, 218–222. http://www.ncbi.nlm.nih.gov/pubmed/10985952.

37. Ruella, M., Xu, J., Barrett, D.M., Fraietta, J.A., Reich, T.J., Ambrose, D.E., Klichinsky, M., Shestova, O., Patel, P.R., Kulikovskaya, I., et al. (2018). Induction of resistance to chimeric antigen receptor T cell therapy by transduction of a single leukemic B cell. Nat. Med. *24*, 1499–1503. http://www.ncbi.nlm.nih.gov/pubmed/30275568.

38. Turtle, C.J., Hanafi, L.-A.A., Berger, C., Gooley, T.A., Cherian, S., Hudecek, M., Sommermeyer, D., Melville, K., Pender, B., Budiarto, T.M., et al. (2016). CD19 CAR-T cells of defined CD4+:CD8+ composition in adult B cell ALL patients. J. Clin. Invest. *126*, 2123–2138. https://doi.org/10.1172/JCI85309. http://www.ncbi.nlm.nih.gov/pubmed/27111235.

39. Braun, C.J., Boztug, K., Paruzynski, A., Witzel, M., Schwarzer, A., Rothe, M., Modlich, U., Beier, R., Göhring, G., Steinemann, D., et al. (2014). Gene therapy for Wiskott-Aldrich syndrome–long-term efficacy and genotoxicity. Sci. Transl. Med. 227ra33. https://doi.org/10.1126/scitranslmed.3007280(227). http://www.ncbi.nlm.nih.gov/pubmed/24622513.

40. Hacein-Bey-Abina, S., Garrigue, A., Wang, G.P., Soulier, J., Lim, A., Morillon, E., Clappier, E., Caccavelli, L., Delabesse, E., Beldjord, K., et al. (2008). Insertional oncogenesis in 4 patients after retrovirus-mediated gene therapy of SCID-X1. J. Clin. Invest. *118*, 3132–3142. http://www.ncbi.nlm.nih.gov/pubmed/18688285.

41. Howe, S.J., Mansour, M.R., Schwarzwaelder, K., Bartholomae, C., Hubank, M., Kempski, H., Brugman, M.H., Pike-Overzet, K., Chatters, S.J., de Ridder, D., et al. (2008). Insertional mutagenesis combined with acquired somatic mutations causes leukemogenesis following gene therapy of SCID-X1 patients. J. Clin. Invest. *118*, 3143–3150. http://www.ncbi.nlm.nih.gov/pubmed/18688286.

42. Ott, M.G., Schmidt, M., Schwarzwaelder, K., Stein, S., Siler, U., Koehl, U., Glimm, H., Kühlcke, K., Schilz, A., Kunkel, H., et al. (2006). Correction of X-linked chronic granulomatous disease by gene therapy, augmented by insertional activation of MDS1-EVI1, PRDM16 or SETBP1. Nat. Med. *12*, 401–409. http://www.ncbi.nlm.nih.gov/pubmed/16582916.

43. Raper, S.E., Chirmule, N., Lee, F.S., Wivel, N.A., Bagg, A., Gao, G.P., Wilson, J.M., and Batshaw, M.L. (2003). Fatal systemic inflammatory response syndrome in a ornithine transcarbamylase deficient patient following adenoviral gene transfer. Mol. Genet. Metab. *80*, 148–158. https://doi.org/10.1016/j.ymgme.2003.08.016. http://www.ncbi.nlm.nih.gov/pubmed/14567964.

44. Stein, S., Ott, M.G., Schultze-Strasser, S., Jauch, A., Burwinkel, B., Kinner, A., Schmidt, M., Krämer, A., Schwäble, J., Glimm, H., et al. (2010). Genomic instability and myelodysplasia with monosomy 7 consequent to EVI1 activation after gene therapy for chronic granulomatous disease. Nat. Med. *16*, 198–204. http://www.ncbi.nlm.nih.gov/pubmed/20098431.

45. Booth, C., Gaspar, H.B., and Thrasher, A.J. (2016). Treating immunodeficiency through HSC gene therapy. Trends Mol. Med. *22*, 317–327. http://www.ncbi.nlm.nih.gov/pubmed/26993219.

46. Milone, M.C., and O'Doherty, U. (2018). Clinical use of lentiviral vectors. Leukemia *32*, 1529–1541. https://doi.org/10.1038/s41375-018-0106-0. http://www.ncbi.nlm.nih.gov/pubmed/29654266.

47. Cornetta, K., Duffy, L., Turtle, C.J., Jensen, M., Forman, S., Binder-Scholl, G., Fry, T., Chew, A., Maloney, D.G., and June, C.H. (2018). Absence of replication-competent lentivirus in the clinic: analysis of infused T cell products. Mol. Ther. *26*, 280–288. http://www.ncbi.nlm.nih.gov/pubmed/28970045.

48. Marcucci, K.T., Jadlowsky, J.K., Hwang, W.T., Suhoski-Davis, M., Gonzalez, V.E., Kulikovskaya, I., Gupta, M., Lacey, S.F., Plesa, G., Chew, A., et al. (2018). Retroviral and lentiviral safety analysis of gene-modified T cell products and infused HIV and oncology patients. Mol. Ther. *26*, 269–279. https://doi.org/10.1016/j.ymthe.2017.10.012.

49. Zufferey, R., Nagy, D., Mandel, R.J., Naldini, L., and Trono, D. (1997). Multiply attenuated lentiviral vector achieves efficient gene delivery in vivo. Nat. Biotechnol. *15*, 871–875. https://doi.org/10.1038/nbt0997-871.

50. Naldini, L., Blömer, U., Gallay, P., Ory, D., Mulligan, R., Gage, F.H., Verma, I.M., and Trono, D. (1996). In vivo gene delivery and stable transduction of nondividing cells by a lentiviral vector. Science *272*, 263–267. https://doi.org/10.1126/science.272.5259.263.

51. Dull, T., Zufferey, R., Kelly, M., Mandel, R.J., Nguyen, M., Trono, D., and Naldini, L. (1998). A third-generation lentivirus vector with a conditional packaging system. J. Virol. *72*, 8463–8471. http://www.ncbi.nlm.nih.gov/pubmed/9765382.